ChemComm

COMMUNICATION

View Article Online
View Journal | View Issue

Cite this: *Chem. Commun.*, 2025, **61**, 12562

Received 16th June 2025,
Accepted 15th July 2025

DOI: 10.1039/d5cc03405a

rsc.li/chemcomm

Scalable one-step syntheses of aluminium-based MOFs†

Miriam Perbet,[a] Thomas Michon,[b] Elsje Alessandra Quadrelli,[a] Mickaële Bonneau *[a] and David Farrusseng [a]

MOF manufacture consists of multistep processes, including filtration and washing steps to remove coproduced salts and wash out the solvent, if any. This constitutes a productivity bottleneck, together with significant costs for waste disposal. We show here a robust single-step route for the synthesis of aluminium-based MOFs that has been successfully applied to Al-fum, MIL-96, MIL-120, and MIL-160, all using aluminium alkoxide as a precursor. Highly crystalline MOFs are obtained with high yields (>90%). No wash-up or separate drying steps are necessary.

As the demand for sustainable and efficient material syntheses increases,[1] researchers are actively exploring synthesis methods for aluminium-based metal–organic frameworks (Al-MOFs). These Al-MOFs are identified as potential candidates for various sorption-related applications, such as water harvesting, CO_2 capture, heat management, environmental remediation...[2–6] The use of earth-abundant aluminium and the availability of a wide variety of industrially produced organic linkers make this Al-MOF family particularly attractive. Al-MOFs show excellent stability towards humidity (high valence metal ions like Al^{3+} present strong bonds with carboxylate linkers according to the hard–soft acid–base principle), making them suitable for multi-ton scale production.[7] Nevertheless, a non-negligible number of challenges remain, among them the widespread use of hazardous solvents and the need for thorough filtering and washing steps to treat coproducts (energy-intensive and time-consuming).[8,9] These challenges hinder the scalability of Al-MOF production and limit their applications in industrial settings.

So far, the best scalable syntheses of Al-MOFs reported in the literature focus on the use of water as a solvent but neglect the production of undesired coproducts (Table S1, ESI†). The MIL-53 synthesis published by P. A. Bayliss *et al.* reports a 500 g scale continuous flow synthesis using $Al(NO_3)_3{\cdot}xH_2O$ and Na-functionalised BDC in water at 300 °C. Unreacted linker is extracted from the final product using supercritical ethanol, which is energy intensive and involves the treatment of salt waste.[10] Concerning CAU-10-H and MIL-160, Z. Zheng *et al.* reported a several kg scale route using 50 L of water with the addition of sodium hydroxide and using, respectively, aluminium sulphate and aluminium chloride as the metal source. The product is filtered and washed with water to remove the produced salt, which involves waste treatment.[2] For MIL-96, M. Benzaqui *et al.* reported two syntheses in water, based on $Al(NO_3)_3{\cdot}xH_2O$, either microwave-assisted with the addition of acetic acid or under reflux conditions. Both synthesised materials are washed with water to remove the produced salt and acid present in the reaction liquor.[11] A solvent-free synthesis is also reported by B. González-Santiago *et al.*, using $Al(NO_3)_3{\cdot}xH_2O$ in a Teflon-lined autoclave at 190 °C, which is harder to scale up and energy demanding compared to the previous synthesis.[12] Finally, MIL-120 has been synthesised using aluminium hydroxy acetate, at a gram scale in water only (80 °C, 72 h) and at a kg scale (reflux, 24 h). This synthesis generates acetic acid as a coproduct, which needs to be neutralised. The final product is washed with hot water to again remove the produced salt.[6]

Recently, we developed a novel, scalable synthesis of aluminium fumarate (Al-fum) based on Al-isopropoxide, a commodity chemical.[13] The dual role of aluminium isopropoxide as a basic and chelating agent enables a steady reaction with fumaric acid without requiring pH adjustment. Unlike previously reported aqueous-phase pathways,[14] this exclusive water-based synthesis (in contrast to NaOH addition[15]) does not require filtering and/or washing steps, as no salts are coproduced. The released isopropanol is removed at the activation step together with the water. The challenge is to assess the efficiency of this single-step, scalable Al-alkoxide-based sol–gel approach on other Al-MOFs with yields approaching 100%.

[a] *Université Claude Bernard Lyon 1, CNRS, IRCELYON, UMR 5256, 2 Av. Albert Einstein, 69626 Villeurbanne cedex, France.*
E-mail: mickaele.bonneau@ircelyon.univ-lyon1.fr
[b] *Axel'One, Rond-point de l'échangeur, Les Levées, 69360 Solaize, France*

† Electronic supplementary information (ESI) available: Details of experimental procedures and characterizations (PXRD, physisorption, TGA). See DOI: https://doi.org/10.1039/d5cc03405a

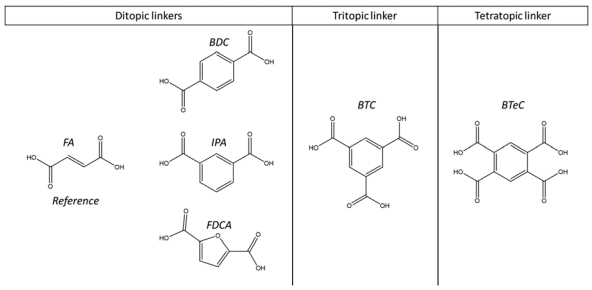

Fig. 1 Schematic structure of di-, tri- and tetratopic linkers (in protonated form) used in this study.

This study reports the extension of the above-mentioned environmentally friendly synthetic route to other Al-MOFs. In this work, only commercially produced and widely available carboxylic acids are evaluated as linkers. In analogy with the reported fumaric acid (FA) used as a reference herein, the following five other organic linkers are tested: 1,4-benzenedicarboxylic acid (BDC), isophthalic acid (IPA), 2,5-furandicarboxylic acid (FDCA), 1,3,5-benzenetricarboxylic acid (BTC) and 1,2,4,5-benzenetetracarboxylic acid (BTeC) (Fig. 1). When combined to aluminium-nodes, they respectively lead to: MIL-53, CAU-10-H, MIL-160, MIL-96 and MIL-120 (Fig. 2). Similarly to Al-fum, three of the above-listed Al-MOFs are based on dicarboxylic linkers: BDC, IPA and FDCA. Both carboxyl groups of those linkers are connected to an organyl group consisting of an aromatic ring, either a benzene or a furan-type ring. Subsequently, a tritopic linker – deprotonated BTC – and a tetratopic linker – deprotonated BTeC – are tested.

Here, we applied the recent protocol developed for Al-fum to the five aforementioned Al-MOFs. As for Al-fum, all syntheses are performed in water with no addition of basic or acidic modulators. The synthesis only contains the appropriate stoichiometric equivalent of metal and linker with a dry mass content of 2.7 wt% (with respect to precursors, Table S2, ESI†).

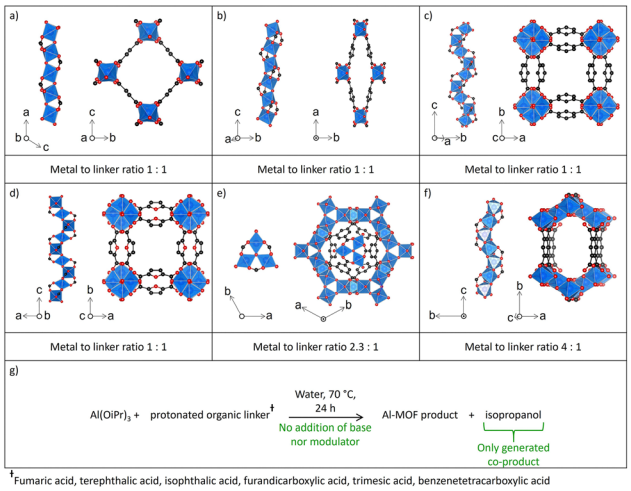

Fig. 2 (a)–(f) Structures of Al-MOFs (Al-fum (a), MIL-53 (b), CAU-10-H (c), MIL-160 (d), MIL-96 (e), and MIL-120 (f)) and the associated Al to organic linker molar ratios. (g) Synthetic approach for the synthesis of Al-MOFs.

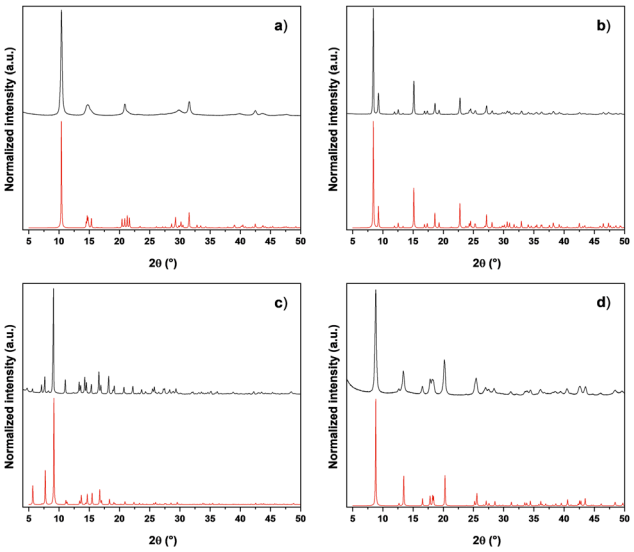

Fig. 3 PXRD patterns of simulated (in red) and as-synthesised (in black) Al-fum (a), MIL-160 (b), MIL-96 (c), and MIL-120 (d) samples.

To maximise the solubility of all linkers in water, all reactions are performed under reflux (T = 100 °C). First, the organic linker and solvent are placed in the heated oil bath, and agitation is set to 500 rpm. When maximum solubilisation is reached, aluminium isopropoxide is added to the mixture. After 24 hours, the synthesised Al-MOF is collected *via* centrifugation and placed in an oven at 70 °C overnight.

Al-fum, MIL-160, MIL-96, and MIL-120 are directly obtained as white powders. The crude materials are all crystalline and their PXRD are in excellent agreement with the calculated patterns obtained from Al-fum, MIL-160, MIL-96, and MIL-120 crystal structures (Fig. 3), with no further washing needed. The permanent porosity of these four Al-MOFs is measured by nitrogen (N_2) adsorption–desorption isotherms at 77 K (Fig. S1, ESI†). All isotherm profiles are reversible and show BET surface areas between 325 and 1100 $m^2\ g^{-1}$ and total pore volumes between 0.24 and 0.58 $cm^3\ g^{-1}$, in line with the theoretical values from the literature (Table 1). CO_2 sorption is measured on MIL-96 and MIL-120 at 298 K, showing an uptake of 2.5 and 2.8 mmol g^{-1}, respectively (Fig. S2, ESI†). TGA analysis under air shows that Al-fum, MIL-160, MIL-96, and MIL-120 are all thermally stable up to at least 300 °C (Fig. S3, ESI†).

Following the successful results obtained through spray-drying for large-scale synthesis of Al-fum,[13] a pilot-scale spray-drying is attempted to produce several kilograms of MIL-160. Among the three candidates, MIL-160 is selected because no polymorphs are expected (unlike MIL-96), and the large-scale purchase of FDCA is cheaper than BTeC. The precursor solution for spray drying is prepared by adding 61.7 kg of aluminium isopropoxide, 47.0 kg of FDCA, and 110 L of water together in a 200 L reactor, corresponding to 49.7 wt% of dry mass (with respect to precursors). After mechanical agitation at 70 °C for 12 hours, the mixture is spray-dried at a flow rate of 69.5 ± 0.5 kg h^{-1}. Details of the spray-drying apparatus and specifics are reported in our previous work.[13] 57 kg of MIL-160

Table 1 Yield ranges, measured and theoretical BET surface areas, and total pore volumes of all as-synthesised materials

Al-MOF	Yield[a] (%)	Measured S_{BET} ($m^2\ g^{-1}$)	S_{BET} ranges in literature ($m^2\ g^{-1}$)	V_{porous} ($cm^3\ g^{-1}$, at p/p_0 = 0.90)
Al-fum[b]	75–90	1078	723–1333[15]	0.54
Al-fum_SP[c]	97[d]	1020		0.52
MIL-160[b]	60–80	1076	968–1180[15]	0.40
MIL-160_SP[c]	96	1135		0.44
MIL-96[b]	90–>98	325	310–600[11,16,17]	0.21
MIL-120[b]	>98	378	308[18]	0.31

[a] Details on the yield measurement are given in the ESI (Table S2). [b] Yields are complicated to calculate accurately for gram-scale syntheses. Yields calculated on scaled-up materials are both more accurate and reliable. [c] SP stands for spray-dried. [d] Yield calculated from precursor and product masses given by M. Perbet *et al.*[13]

are collected, which represents a yield of 96% if we consider the material to be recovered dehydrated (Table 1). PXRD pattern, nitrogen adsorption isotherm and the SEM images of the sample confirmed the good quality of MIL-160 similar to the lab scale synthesis (Fig. 4 and Fig. S4, ESI†).

In summary, the extension of the Al-fum scalable synthesis has been successfully applied to MIL-160, MIL-96, and MIL-120; among these three, the first was successfully scaled up through spray-drying up to about 60 kg. All syntheses are repeatable with the same properties. The same approach is attempted with BDC and IPA. Conversely, the crude materials obtained show a different phase than the simulated PXRD patterns for MIL-53 and CAU-10-H, the targeted materials. Both samples are washed with ethanol (using a Soxhlet), and a second PXRD analysis is performed. Differences between the first and second patterns reveal that some peaks of MIL-53 are due to the remaining linker. In the case of CAU-10-H, no proof of remaining linker is detected, but rather an unknown phase, different from the expected pattern (Fig. S5, ESI†). The N_2 physisorptions measured on both samples show little to no porosity (Fig. S1, ESI†).

At first glance, it is not easy to determine the parameters that influence the Al-MOF formation. First, differences in topology are not a relevant parameter. Indeed, all mentioned Al-MOFs are built from Al^{3+} ions coordinated by six oxygen atoms, forming [AlO_6] octahedra as their primary inorganic building unit. These octahedra are connected *via* hydroxyl bridges (μ_2-OH or μ_3-O), water molecules, or directly through carboxylate groups from the organic linkers. All MOFs except MIL-96 adopt infinite chains, whereas MIL-96 combines isolated trimers with infinite chains.[18–24] Al-fum and MIL-53 are isoreticular with ditopic ligands, with the exception that Al-fum possesses rigid channels, whereas MIL-53 is flexible upon external stimuli. MIL-160 and CAU-10-H are also isoreticular, with different pore sizes. All these MOFs have an Al/linker ratio of 1 to 1 according to their formula. MIL-53 and CAU-10-H synthesis attempts failed even though the structures are isoreticular to successfully synthesised Al-fum and MIL-160, respectively. MIL-96 and MIL-120 are 3D structures based on tritopic and tetratopic and present an Al/ligand ratio of 2.3 to 1 and 4 to 1, respectively.

Moreover, the linker's solubility in water is a critical factor, which directly affects the pH. pH values are measured at the beginning (only water plus organic linker) and after 24 hours of reaction (Fig. 5 and Fig. S6, Table S4, ESI†) to get an insight into the reagent's consumption. A trend is observed between the starting pH and the synthesis success: the syntheses with the lowest pH at the start are those that work. The possible influence of the pH limits at the reaction start is tightly linked to the acid's solubility in the reaction media (Table S5, ESI†). At higher starting pH, aluminium isopropoxide is partially hydrolysed to available Al^{3+}. Indeed, according to B. Lekhlif *et al.*, the predominance of Al^{3+} species in acidic media is assessed until pH = 3.5.[25] No formation of aluminium hydroxide is observed in all our syntheses (pH starting value for aluminium hydroxide formation being about 4.25, Fig. 5). The non-formation of MIL-53 and CAU-10-H phases, for which the pH at the start is 4.00 (out of Al^{3+} predominance zone) and 3.48 (limit of Al^{3+} predominance zone), indicates that linker deprotonation impacts

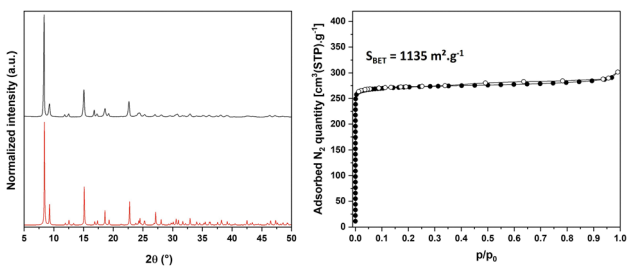

Fig. 4 PXRD pattern (left) and N_2 adsorption/desorption isotherm at 77 K (right) of the pilot batch spray-dried MIL-160 sample.

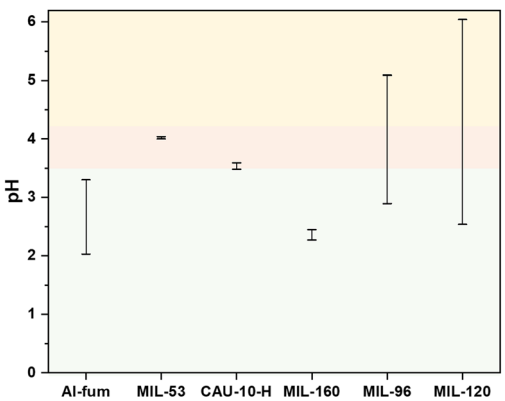

Fig. 5 pH ranges of all syntheses (first point at reaction start and second after 24 hours). The green zone represents the predominance of Al^{3+} species, the red zone is an in-between where plural ionic species exist, and the yellow one is the limit from which aluminium hydroxide starts forming.

al-isopropoxide hydrolysis. It is also interesting to notice that between the start and end of the reaction for MIL-53 and CAU-10-H syntheses, there is almost no pH variation. This could reflect the low reactivity between Al^{3+} and the linker.

It is important to recall that key features of the studied reaction pathway are the exclusive use of water as the solvent, without any addition of base or modulating agents, allowing also the suppression of washing steps, making it a one-step synthesis. We demonstrate that Al-fum, MIL-160, MIL-96, and MIL-120, which are promising for CO_2 capture and water-related sorption applications, are obtained through this reported scalable synthesis pathway at high yield and without compromising product quality (high crystallinity and expected surface areas). Scale-up *via* spray-drying is herein demonstrated on MIL-160 (57 kg in one batch, yield 96%), showing that this one-step scalable synthesis is robust to linker change. This opens an easy and sustainable path towards an industrial process for large-scale Al-MOF production. Further mechanistic studies on Al-MOFs are under progress to reveal the formation of these porous materials as well as the economic impact of such synthesis for the production of Al-MOF at large scale.

This project has received funding from the European Union's Horizon 2020 research and innovation program under grant agreement no. 101058565 (AMBHER project), funded by the European Union. Views and opinions expressed are however those of the author(s) only and do not necessarily reflect those of the European Union. Neither the European Union nor the granting authority can be held responsible for them. We would also like to thank MOFapps for their financial support.

Conflicts of interest

There are no conflicts to declare.

Data availability

The data supporting this article, including physisorption data in AIF format, have been included as ESI.†

Notes and references

1 Z. Xie and J. Hou, *Ind. Eng. Chem. Res.*, 2025, **64**, 7941–7955.
2 Z. Zheng, A. H. Alawadhi and O. M. Yaghi, *Mol. Front. J.*, 2023, **07**, 20–39.
3 H. Kummer, F. Jeremias, A. Warlo, G. Füldner, D. Fröhlich, C. Janiak, R. Gläser and S. K. Henninger, *Ind. Eng. Chem. Res.*, 2017, **56**, 8393–8398.
4 E. Moumen, L. Bazzi and S. El Hankari, *Process Saf. Environ. Prot.*, 2022, **160**, 502–512.
5 F. Jeremias, D. Fröhlich, C. Janiak and S. K. Henninger, *RSC Adv.*, 2014, **4**, 24073–24082.
6 B. Chen, D. Fan, R. V. Pinto, I. Dovgaliuk, S. Nandi, D. Chakraborty, N. García-Moncada, A. Vimont, C. J. McMonagle, M. Bordonhos, A. Al Mohtar, I. Cornu, P. Florian, N. Heymans, M. Daturi, G. De Weireld, M. Pinto, F. Nouar, G. Maurin, G. Mouchaham and C. Serre, *Adv. Sci.*, 2024, **11**, 2401070.
7 R. G. Pearson, *J. Chem. Educ.*, 1968, **45**, 581.
8 A. Czaja, E. Leung, N. Trukhan and U. Müller, in *Metal-Organic Frameworks*, ed. D. Farrusseng, Wiley, 1st edn, 2011, pp. 337–352.
9 E. Gkaniatsou, C. Chen, F. S. Cui, X. Zhu, P. Sapin, F. Nouar, C. Boissière, C. N. Markides, J. Hensen and C. Serre, *Cell Rep. Phys. Sci.*, 2022, **3**, 100730.
10 P. A. Bayliss, I. A. Ibarra, E. Pérez, S. Yang, C. C. Tang, M. Poliakoff and M. Schröder, *Green Chem.*, 2014, **16**, 3796–3802.
11 M. Benzaqui, R. S. Pillai, A. Sabetghadam, V. Benoit, P. Normand, J. Marrot, N. Menguy, D. Montero, W. Shepard, A. Tissot, C. Martineau-Corcos, C. Sicard, M. Mihaylov, F. Carn, I. Beurroies, P. L. Llewellyn, G. De Weireld, K. Hadjiivanov, J. Gascon, F. Kapteijn, G. Maurin, N. Steunou and C. Serre, *Chem. Mater.*, 2017, **29**, 10326–10338.
12 B. González-Santiago, A. García-Carrillo, L. Chávez-Guerrero, M. Poisot, A. A. Lemus-Santana, M. Á. García-Sánchez and O. Medina-Juárez, *Inorg. Chem. Commun.*, 2023, **155**, 111095.
13 M. Perbet, T. Aumond, C. Collomb, C. Daniel, I. Imaz, G. Pena, D. Maspoch, T. Michon, R. Morales-Ospino, V. Fierro, E. A. Quadrelli and D. Farrusseng, *Ind. Eng. Chem. Res.*, 2025, **64**, 6541–6549.
14 M. Rubio-Martinez, T. D. Hadley, M. P. Batten, K. Constanti-Carey, T. Barton, D. Marley, A. Mönch, K. Lim and M. R. Hill, *ChemSusChem*, 2016, **9**, 938–941.
15 N. Tannert, C. Jansen, S. Nießing and C. Janiak, *Dalton Trans.*, 2019, **48**, 2967–2976.
16 T. B. Čelič, A. Škrjanc, J. M. Coronado, T. Čendak, V. A. de la Peña O'Shea, D. P. Serrano and N. Zabukovec Logar, *Nanomaterials*, 2022, **12**, 2092.
17 D. Liu, Y. Liu, F. Dai, J. Zhao, K. Yang and C. Liu, *Dalton Trans.*, 2015, **44**, 16421–16429.
18 C. Volkringer, T. Loiseau, M. Haouas, F. Taulelle, D. Popov, M. Burghammer, C. Riekel, C. Zlotea, F. Cuevas, M. Latroche, D. Phanon, C. Knöfelv, P. L. Llewellyn and G. Férey, *Chem. Mater.*, 2009, **21**, 5783–5791.
19 E. Alvarez, N. Guillou, C. Martineau, B. Bueken, B. Van de Voorde, C. Le Guillouzer, P. Fabry, F. Nouar, F. Taulelle, D. de Vos, J.-S. Chang, K. H. Cho, N. Ramsahye, T. Devic, M. Daturi, G. Maurin and C. Serre, *Angew. Chem., Int. Ed.*, 2015, **54**, 3664–3668.
20 A. Cadiau, J. S. Lee, D. Damasceno Borges, P. Fabry, T. Devic, M. T. Wharmby, C. Martineau, D. Foucher, F. Taulelle, C.-H. Jun, Y. K. Hwang, N. Stock, M. F. De Lange, F. Kapteijn, J. Gascon, G. Maurin, J.-S. Chang and C. Serre, *Adv. Mater.*, 2015, **27**, 4775–4780.
21 H. Reinsch, M. A. van der Veen, B. Gil, B. Marszalek, T. Verbiest, D. de Vos and N. Stock, *Chem. Mater.*, 2013, **25**, 17–26.
22 PCT/FR2009/052208, 2010.
23 T. Loiseau, C. Serre, C. Huguenard, G. Fink, F. Taulelle, M. Henry, T. Bataille and G. Férey, *Chem. – Eur. J.*, 2004, **10**, 1373–1382.
24 T. Loiseau, L. Lecroq, C. Volkringer, J. Marrot, G. Férey, M. Haouas, F. Taulelle, S. Bourrelly, P. L. Llewellyn and M. Latroche, *J. Am. Chem. Soc.*, 2006, **128**, 10223–10230.
25 B. Lekhlif, L. Oudrhiri, F. Zidane, P. Drogui and J. F. Blais, *J. Mater. Environ. Sci.*, 2014, **5**, 111–120.